Supplementary Information

Hydrazone-based Boron Difluoride Complexes as Triplet Photosensitizers for Singlet Oxygen Generation

Sven van Vliet, Johannes G. H. Hermens, Youxin Fu, Lukas Pfeifer, Ben L. Feringa*

Stratingh Institute for Chemistry, University of Groningen, Nijenborgh 4, 9747 AG, Groningen, The Netherlands

E-mail: b.l.feringa@rug.nl

Table of contents

S1 Synthesis & Characterization

General Synthetic Procedures

All reactions involving air sensitive reagents were performed under a N_2 atmosphere.
Reagents were purchased from Sigma Aldrich, Acros or TCI Europe and used as received. Solvents were reagent-grade and used without prior water removal unless otherwise indicated. Anhydrous THF was obtained from a solvent purification system (MBraun SPS-800). Thin layer chromatography (TLC) was carried out on aluminium sheets coated with silica gel 60 F254 (Merck). Compounds were visualised with a UV lamp (254 nm) and/or by staining with KMnO4 or Cerium Ammonium Molybdate.

^{1}H and ^{13}C NMR spectra were recorded on a Varian Mercury-Plus 400 or a Bruker Avance 600 NMR spectrometer at 298 K unless otherwise indicated. Chemical shifts are given in parts per million (ppm) relative to the residual solvent signal (for CD_2Cl_2 δ 5.32 for ^{1}H, δ 53.84 for ^{13}C). Multiplets in ^{1}H NMR spectra are designated as follows: s (singlet), d (doublet), t (triplet), q (quartet), p (pentet), m (multiplet), br (broad). High resolution mass spectrometry (ESI+) was performed on an LTQ Orbitrap XL spectrometer.

For experimental details and procedures regarding photooxygenation reactions, see **S5** and **S6**.

Synthetic Procedures

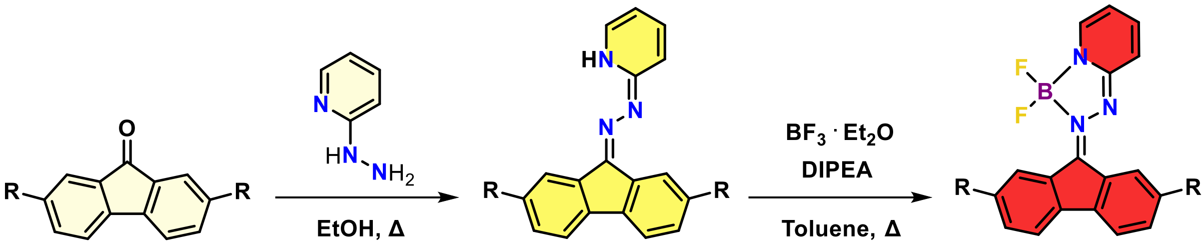

R = H 75% **L1**
Br 78% **L2**

R = H 95% **BH1**
Br 90% **BH2**

General procedure condensation hydrazone ligands L1 & L2

The fluorene-based ketone (1.0 eq) was dissolved in EtOH (0.3 M), 2-hydrazinopyridine (3.0 eq) was added and the mixture was heated at reflux for 16 h. Hereafter, the solution was allowed to reach room temperature and stored in the freezer at -25 °C for several hours to induce crystallization. The resulting crystals were filtered off, washed with a minimal amount of ice cold EtOH and air-dried to obtain the desired hydrazone ligand.

General procedure Boron complexation BH1 & BH2

The aforementioned bidentate hydrazone ligand (1.0 eq) was suspended in anhydrous toluene (0.1 M), whereafter the mixture was heated to 90 °C. Hereafter, BF_3 Et_2O (5.0 eq) and DIPEA (3.0 eq) were added dropwise. The intensely coloured mixture was stirred at 90 °C for 20 h before it was cooled down to room temperature. After cooling down, the mixture was poured onto a Silica plug (10 cm) and washed with toluene until the filtrate became colourless. The organic volatiles were removed in vacuo to obtain the boron difluoride complexes as lustrous solids.

Characterization

(*Z*)-2-((*9*H-fluoren-9-ylidene)hydrazineylidene)-1,2-dihydropyridine **L1**.

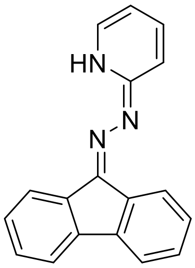

Starting from *9H*-fluoren-9-one (3.06 g, 17.0 mmol), the title compound was obtained as orange crystals (3.45 g, 75%)
^{1}H NMR (400 MHz,CD_2Cl_2) δ 9.39 (br, 1H), 8.24 (d, J = 4.9, 1.9 Hz, 1H), 8.07 (d, J = 7.5, 1.0 Hz, 1H), 7.94 – 7.85 (m, 1H), 7.83 (dt, J = 7.5, 1.0 Hz, 1H), 7.79 – 7.66 (m, 2H), 7.64 (d, J = 8.4, 1.0 Hz, 1H), 7.50 (t, J = 7.5, 1.0 Hz, 1H), 7.40 (m, 3H), 6.94 (ddd, J = 7.2, 4.9, 1.1 Hz, 1H).
^{13}C NMR (400 MHz, CD_2Cl_2) 157.19, 148.25, 141.79, 141.76, 138.86, 138.63, 138.10, 130.36, 130.30, 129.04, 128.27, 128.21, 125.42, 121.27, 121.06, 120.06, 117.64, 107.87.
HRMS (ESI+, m/z) calcd for $C_{18}H_{13}N_3$ [M+H$^+$]= 272.1182, found 272.1175.

(*Z*)-2-((2,7-dibromo-*9*H-fluoren-9-ylidene)hydrazineylidene)-1,2-dihydropyridine **L2**

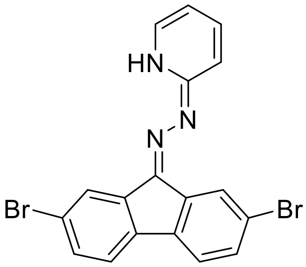

Starting from 2,7-dibromo-9-fluorenone (4.95 g, 14.6 mmol), the title compound was obtained as yellow crystals (4.90 g, 78%)
^{1}H NMR (400 MHz, CD_2Cl_2) δ 9.40 (s, br), 8.26 (ddd, J = 5.0, 1.8, 1.0 Hz, 1H), 8.22 (d, J = 1.6 Hz, 1H), 8.01 (d, J = 1.8 Hz, 1H), 7.78 (m, 1H), 7.70 – 7.59 (m, 3H), 7.58 – 7.47 (m, 2H), 6.99 (ddd, J = 7.3, 5.0, 1.0 Hz, 1H).
^{13}C NMR (600 MHz, CD_2Cl_2) δ 156.25, 147.84, 139.46, 139.11, 138.43, 138.33, 136.16, 132.65, 131.37, 131.16, 127.71, 124.02, 121.99, 121.94, 121.52, 121.18, 117.97, 107.82.
HRMS (ESI+, m/z) calcd for $C_{18}H_{11}Br_2N_3$ [M+H$^+$]= 427.9393, found 427.9384.

2-(*9*H-fluoren-9-ylidene)-3,3-difluoro-2,3-dihydro-2λ^4,3λ^4-[1,2,4,3]triazaborolo[4,5-a]pyridine **BH1**

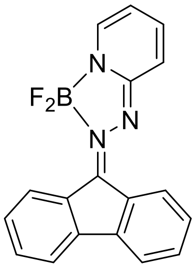

Starting from **L1** (0.737 g, 2.72 mmol), the title compound was obtained as shiny, deep red solid (0.850 g, 95%)

^{1}H NMR (400 MHz, CD_2Cl_2) δ 9.07 (d, *J* = 7.8 Hz, 1H), 8.44 – 8.35 (m, 1H), 7.70 – 7.63 (m, 3H), 7.59 (ddd, *J* = 9.0, 6.8, 1.6 Hz, 1H), 7.48 (td, *J* = 7.6, 1.2 Hz, 1H), 7.40 (dtd, *J* = 14.4, 7.6, 1.2 Hz, 2H), 7.31 (td, *J* = 7.6, 1.2 Hz, 1H), 6.97 (d, *J* = 9.0 Hz, 1H), 6.59 – 6.52 (m, 1H).

^{13}C NMR (600 MHz, CD_2Cl_2) δ 142.30, 141.79, 141.76, 136.12, 132.57, 132.08, 131.51, 129.67, 128.93, 128.59, 126.53, 126.44, 126.34, 120.87, 120.51, 120.10, 113.91, 111.69.

^{19}F NMR (400 MHz, CD_2Cl_2) δ -150.3.

HRMS (ESI+, m/z) calcd for $C_{18}H_{12}BF_2N_3$ [M+H$^+$]= 320.1165, found 320.1159.

2-(2,7-dibromo-*9*H-fluoren-9-ylidene)-3,3-difluoro-2,3-dihydro-2λ^4,3λ^4-[1,2,4,3]triazaborolo[4,5-a]pyridine **BH2**

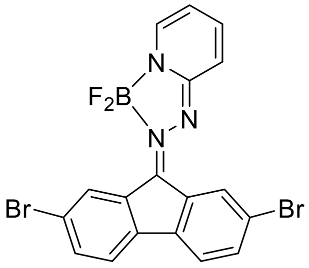

Starting from **L2** (0.495 g, 1.15 mmol), the title compound was obtained as lustrous, purple solid (0.495 g, 90%)

^{1}H NMR (600 MHz, CD_2Cl_2) δ 9.23 (d, J = 1.8 Hz, 1H), 8.51 – 8.47 (m, 1H), 7.78 – 7.66 (m, 2H), 7.62 (d, J = 7.9 Hz, 1H), 7.58 – 7.49 (m, 2H), 7.11 (d, J = 8.9 Hz, 1H), 6.70 (t, J = 6.5 Hz, 1H).

^{13}C NMR (600 MHz, CD_2Cl_2) δ 143.30, 139.22, 136.52, 134.93, 134.06, 133.92, 133.87, 133.79, 133.18, 129.06, 128.99, 128.92, 122.73, 122.45, 121.87, 121.44, 114.40, 113.24.

^{19}F NMR (400 MHz, CD_2Cl_2) δ -150.1.

HRMS (ESI+, m/z) calcd for $C_{18}H_{10}BBr_2F_2N_3$ [M+H$^+$]= 475.9375, found 475.9359.

(*Z*)-2-((9*H*-fluoren-9-ylidene)hydrazineylidene)-1,2-dihydropyridine **L1**.

^{1}H NMR (CD_2Cl_2)

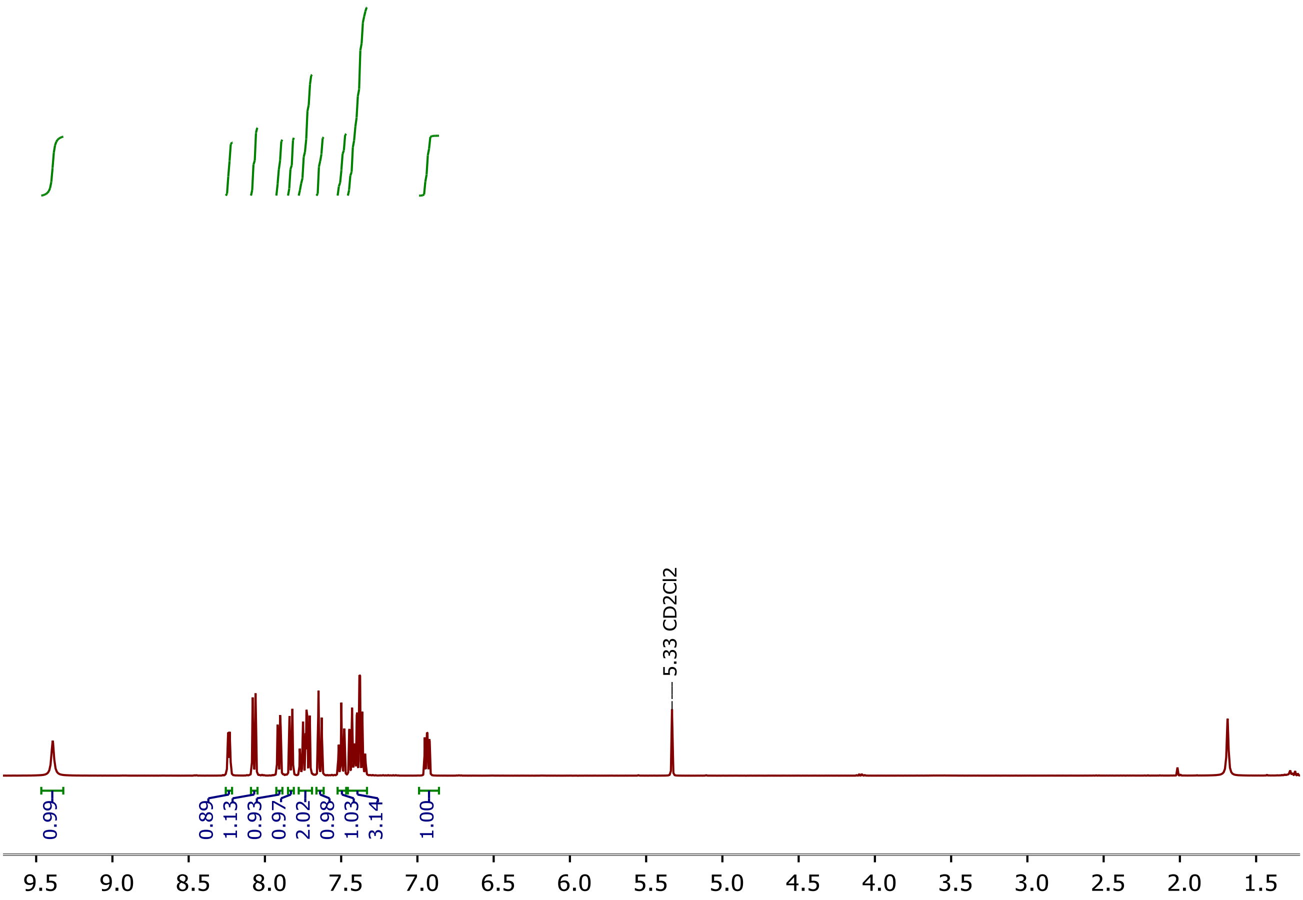

Expansion aromatic region

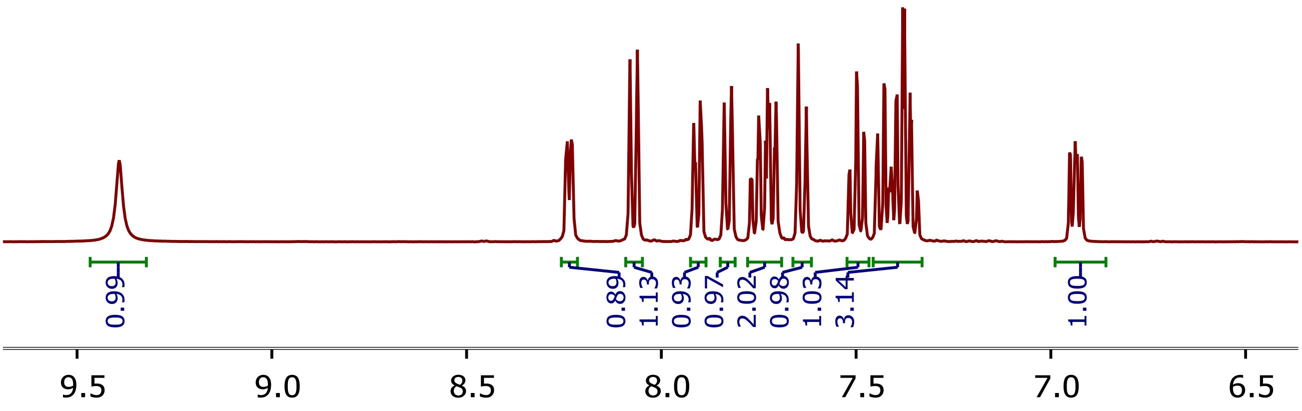

^{13}C NMR (CD$_2$Cl$_2$

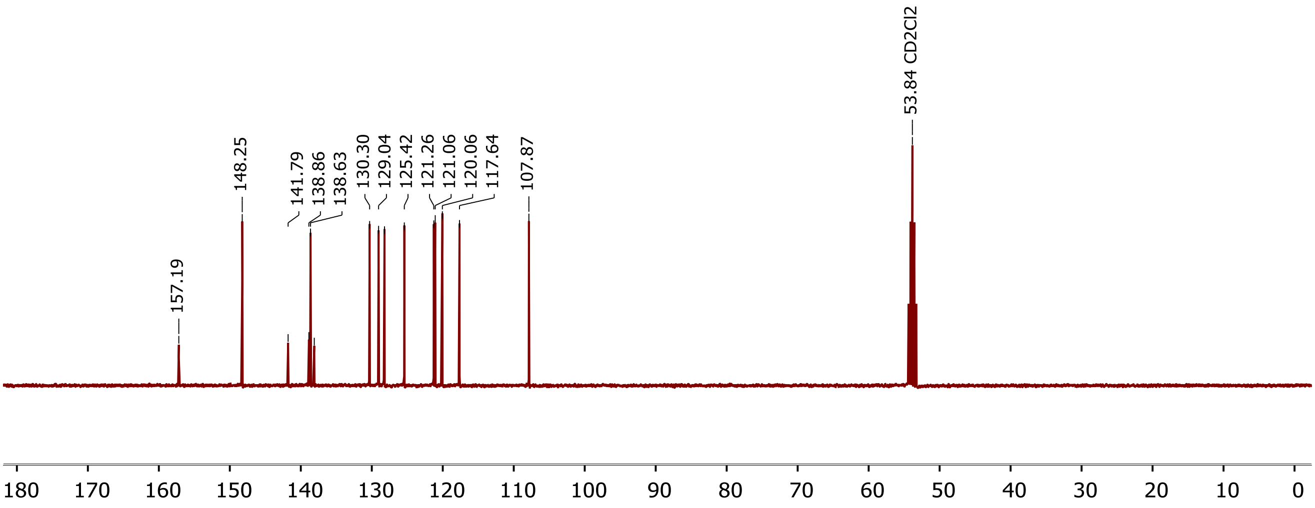

HRMS

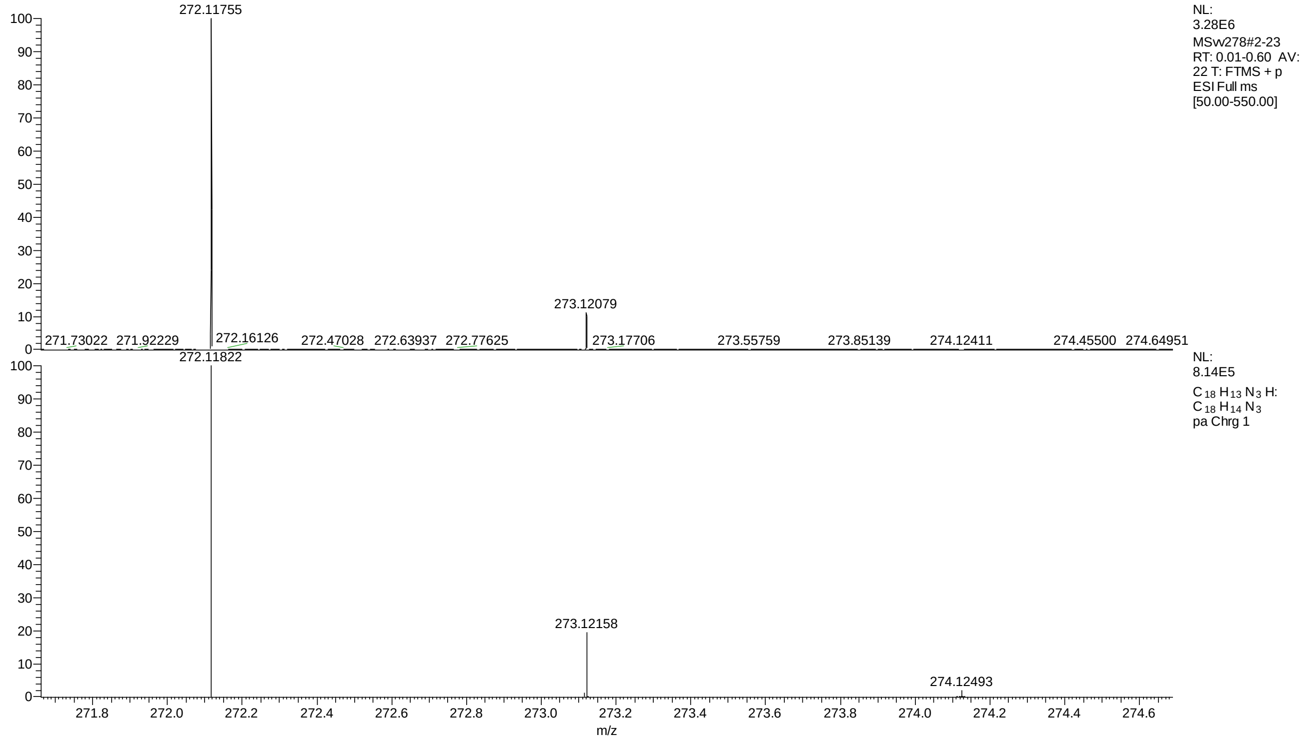

(*Z*)-2-((2,7-dibromo-*9*H-fluoren-9-ylidene)hydrazineylidene)-1,2-dihydropyridine **L2**
^{1}H NMR (CD_2Cl_2)

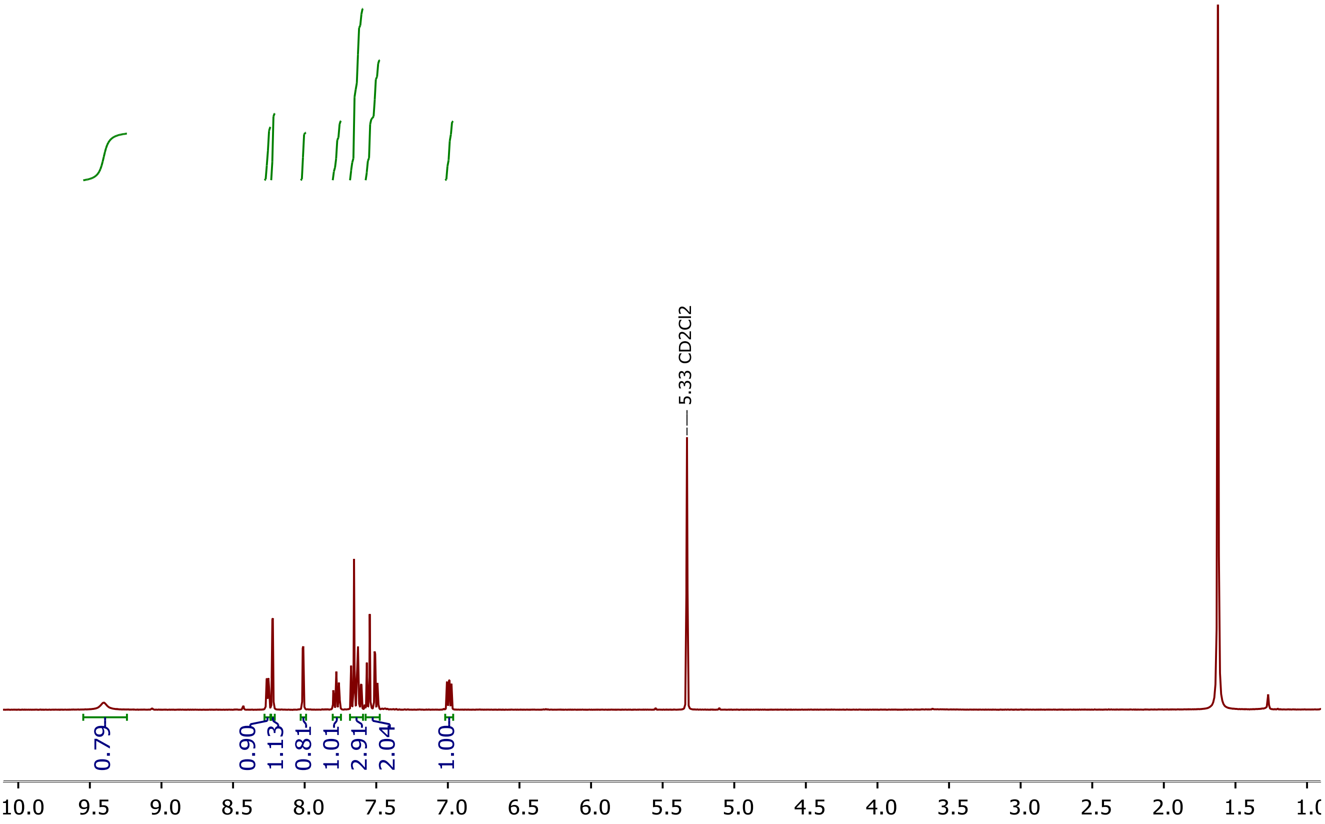

Expansion aromatic region

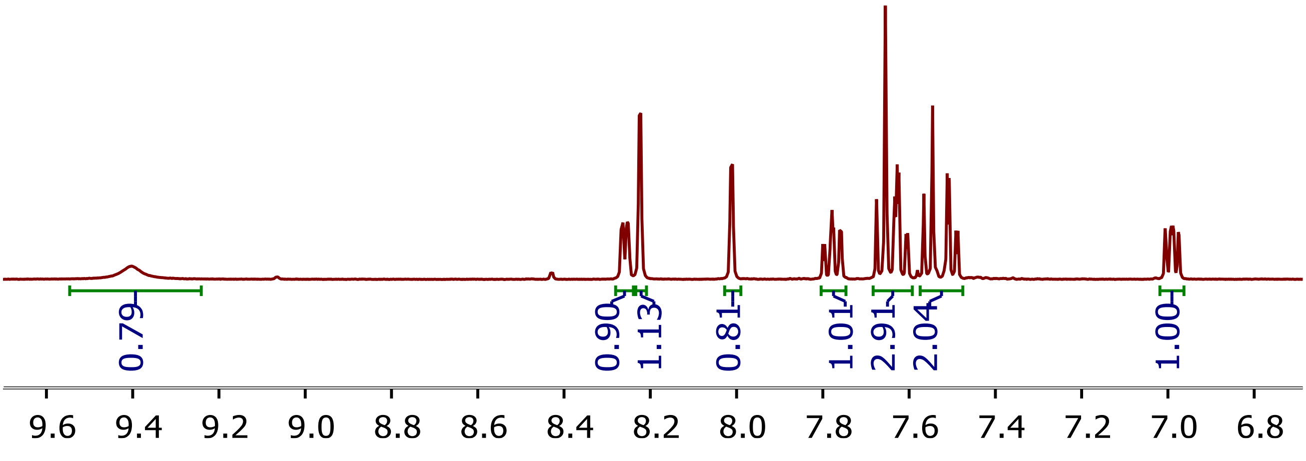

^{13}C NMR (CD_2Cl_2)

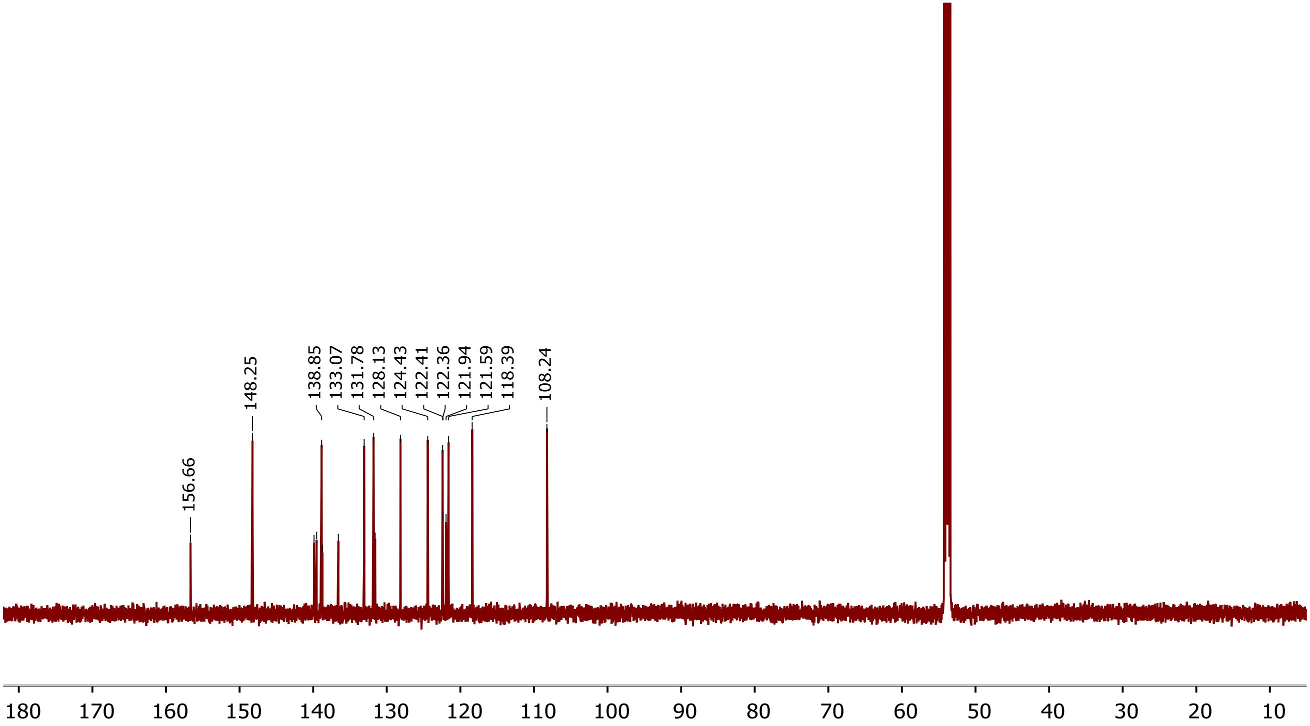

HRMS

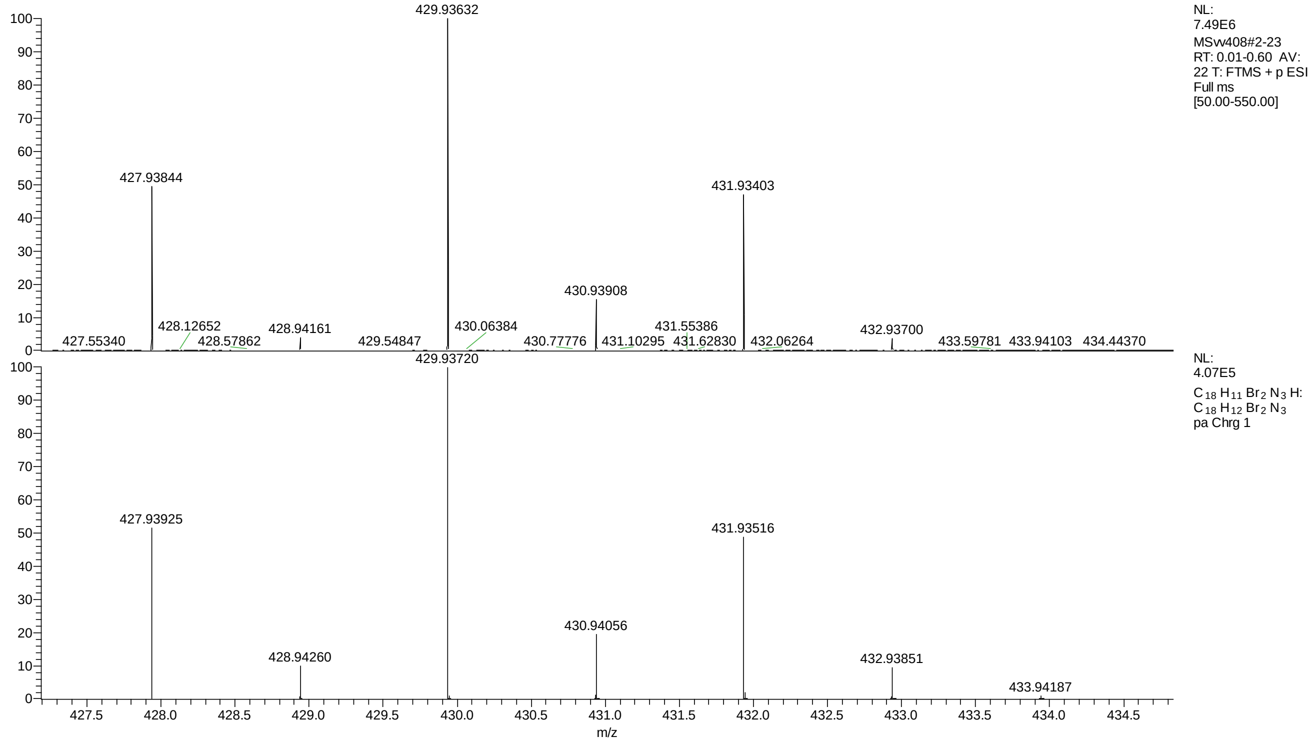

2-(*9*H-fluoren-9-ylidene)-3,3-difluoro-2,3-dihydro-2λ^{4},3λ^{4}-[1,2,4,3]triazaborolo[4,5-a]pyridine **BH1**

^{1}H NMR (CD_2Cl_2)

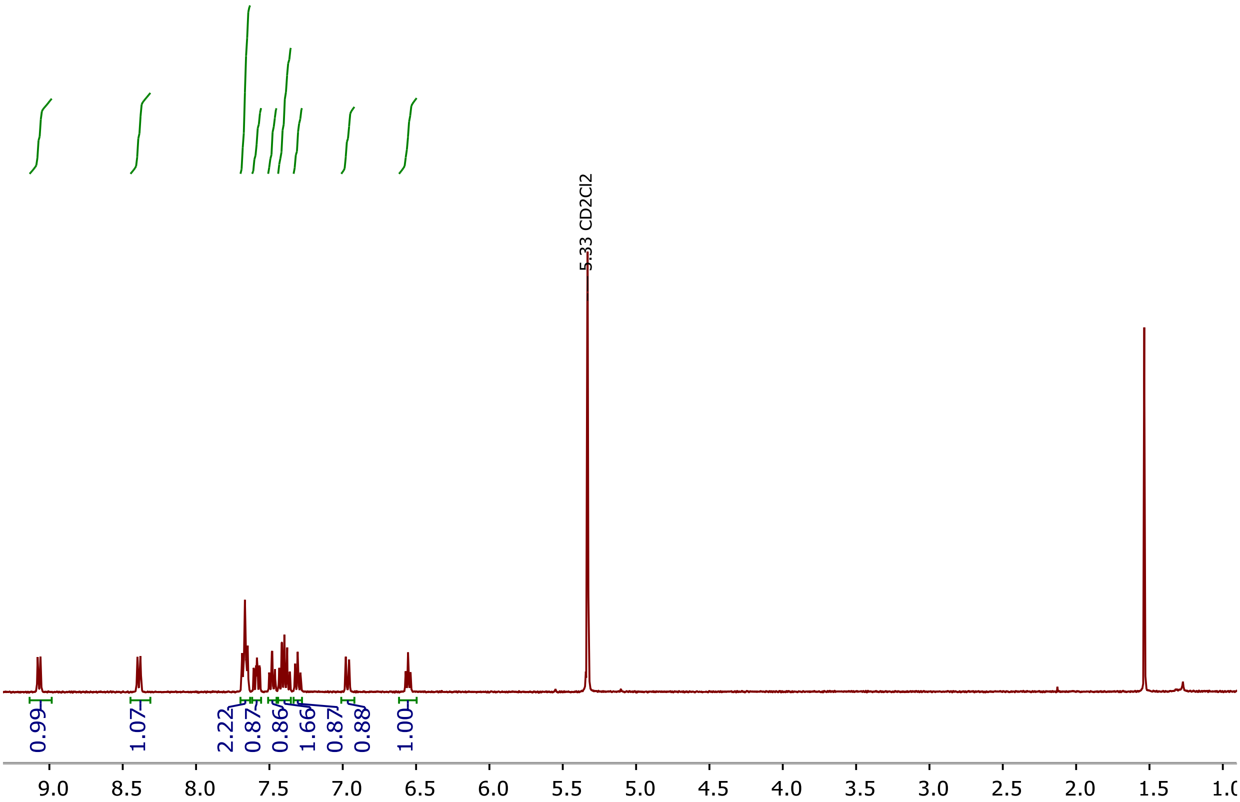

Expansion aromatic region

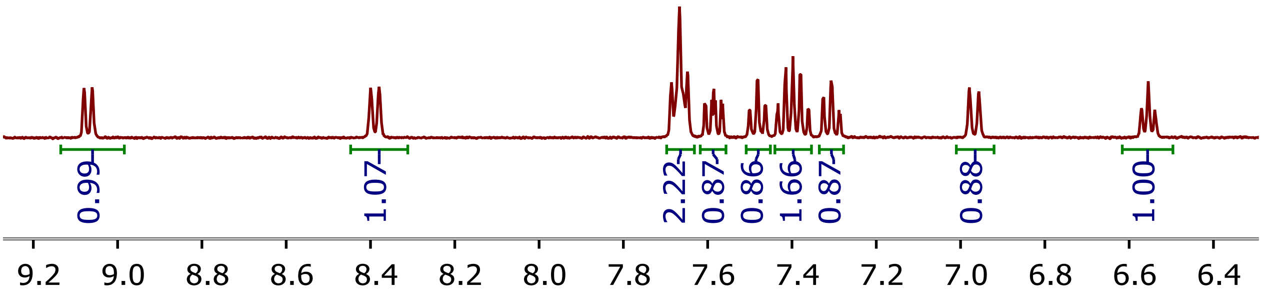

^{13}C NMR (CD_2Cl_2)

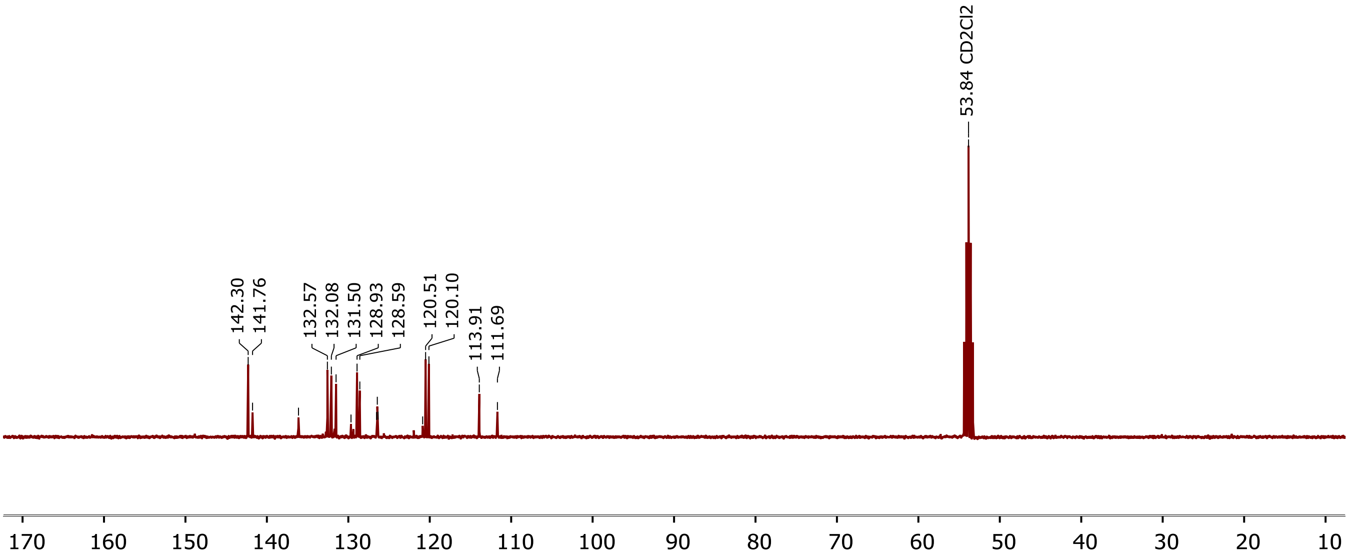

^{19}F NMR (CD_2Cl_2)

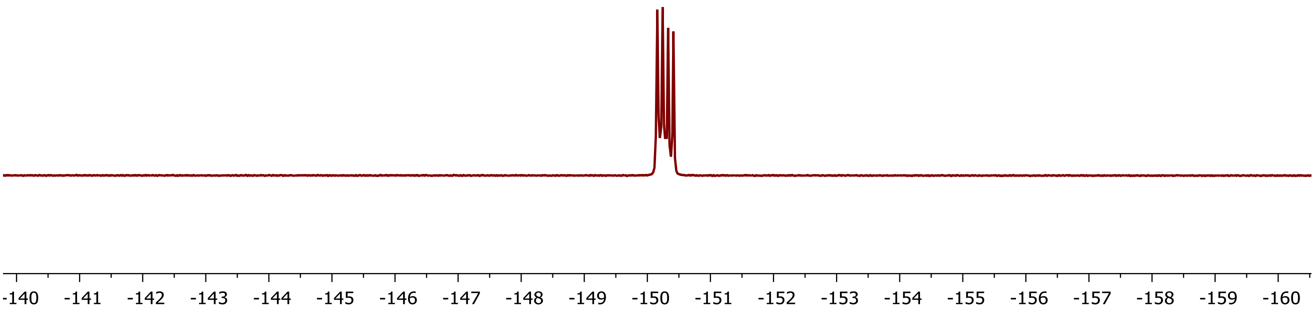

HRMS

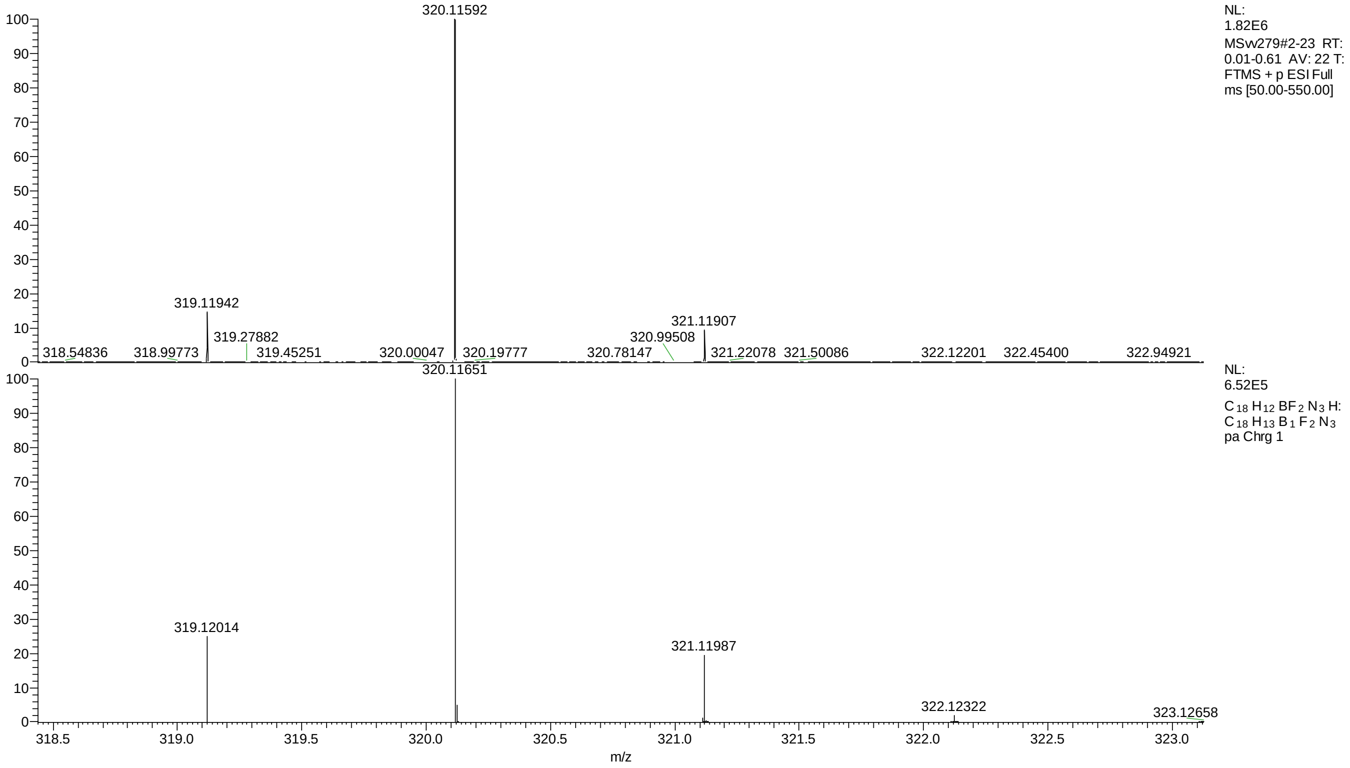

320.11592
NL:
1.82E6
MSw279#2-23 RT:
0.01-0.61 AV: 22 T:
FTMS + p ESI Full
ms [50.00-550.00]
319.11942
321.11907
319.27882
320.99508
318.54836
318.99773
319.45251
320.00047
320.19777
320.78147
321.22078
321.50086
322.12201
322.45400
322.94921
320.11651
NL:
6.52E5
C 18 H 12 BF 2 N 3 H:
C 18 H 13 B 1 F 2 N 3
pa Chrg 1
319.12014
321.11987
322.12322
323.12658
m/z

2-(2,7-dibromo-*9*H-fluoren-9-ylidene)-3,3-difluoro-2,3-dihydro-2λ^4,3λ^4-[1,2,4,3]triazaborolo[4,5-a]pyridine **BH2**

^{1}H NMR (CD_2Cl_2)

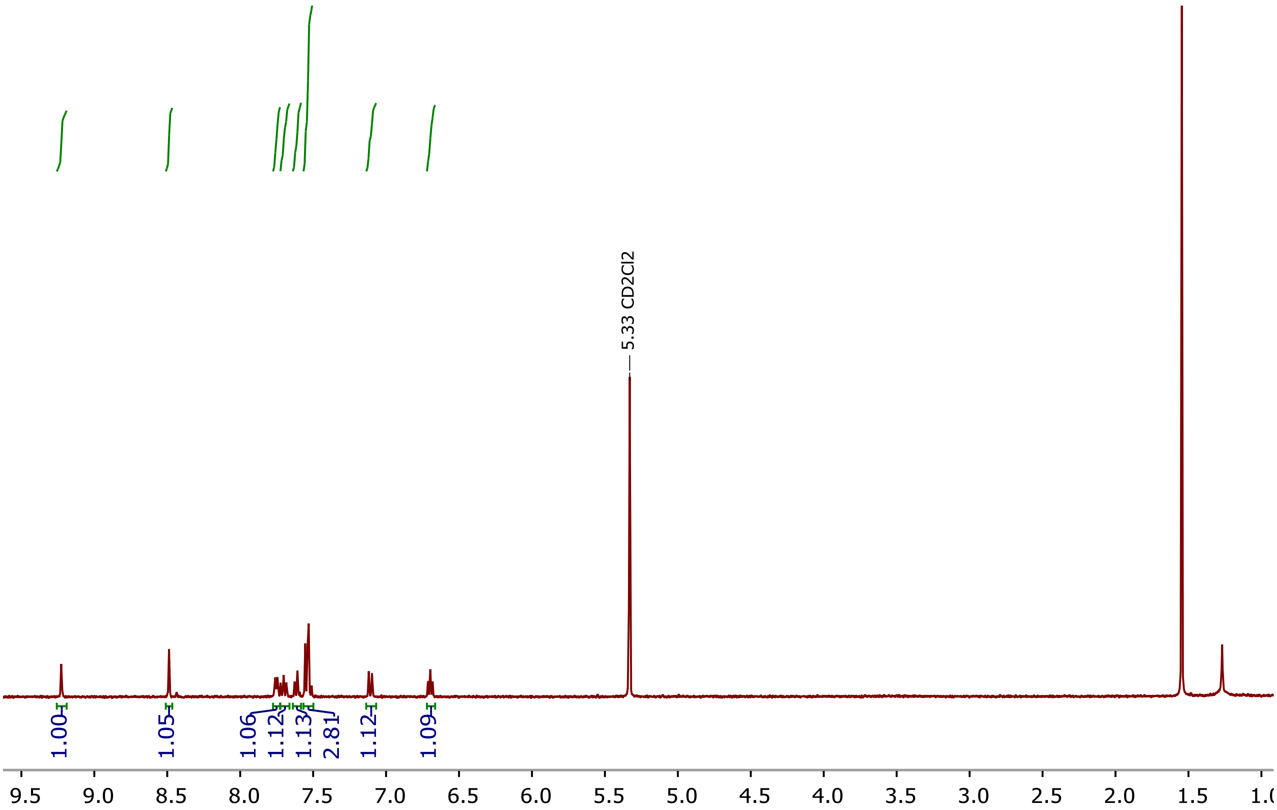

Expansion aromatic region

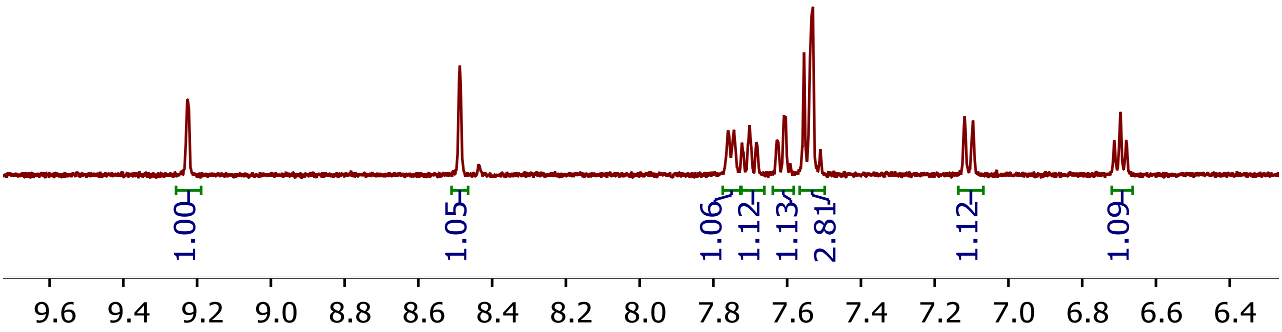

^{13}C NMR (CD$_2$Cl$_2$)

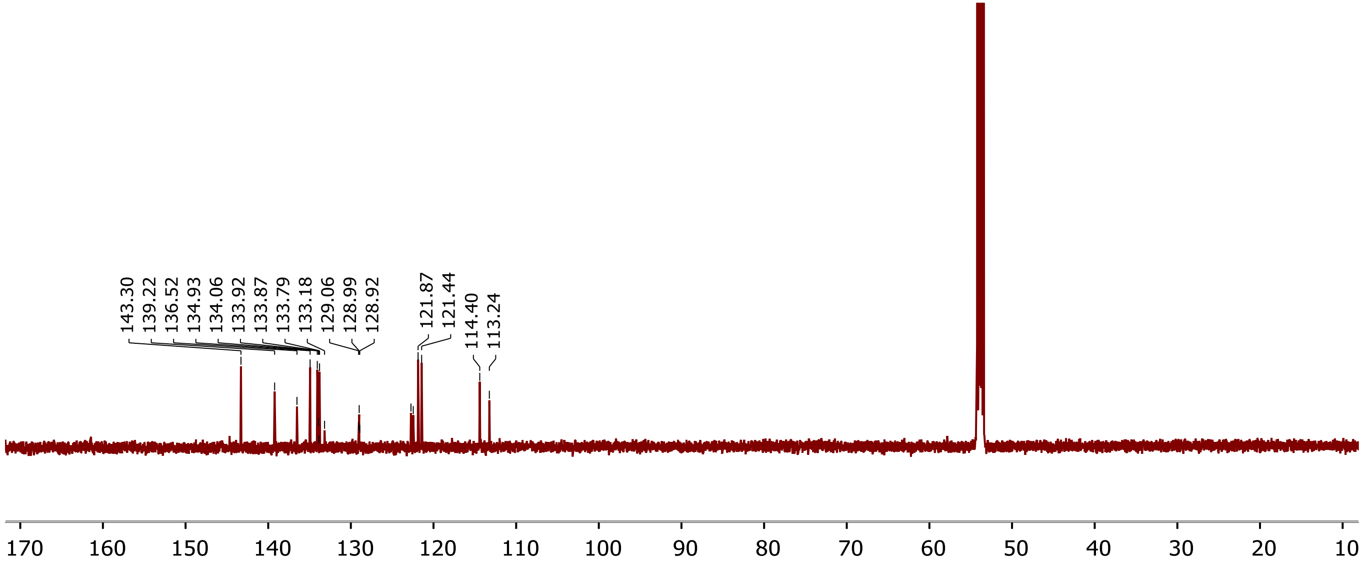

^{19}F NMR (CD$_2$Cl$_2$)

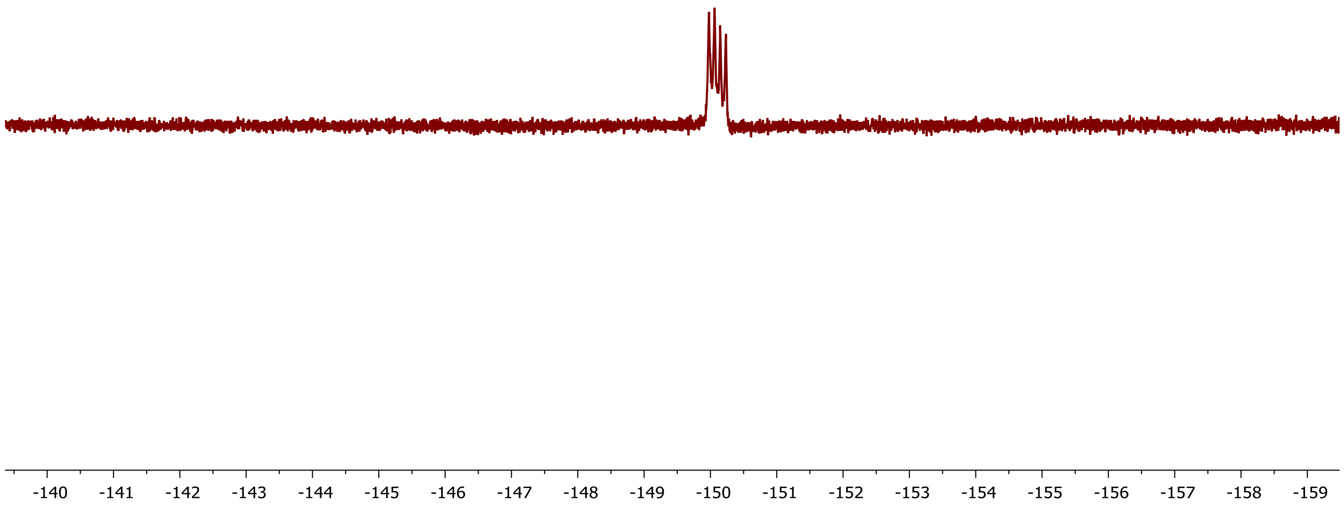

HRMS

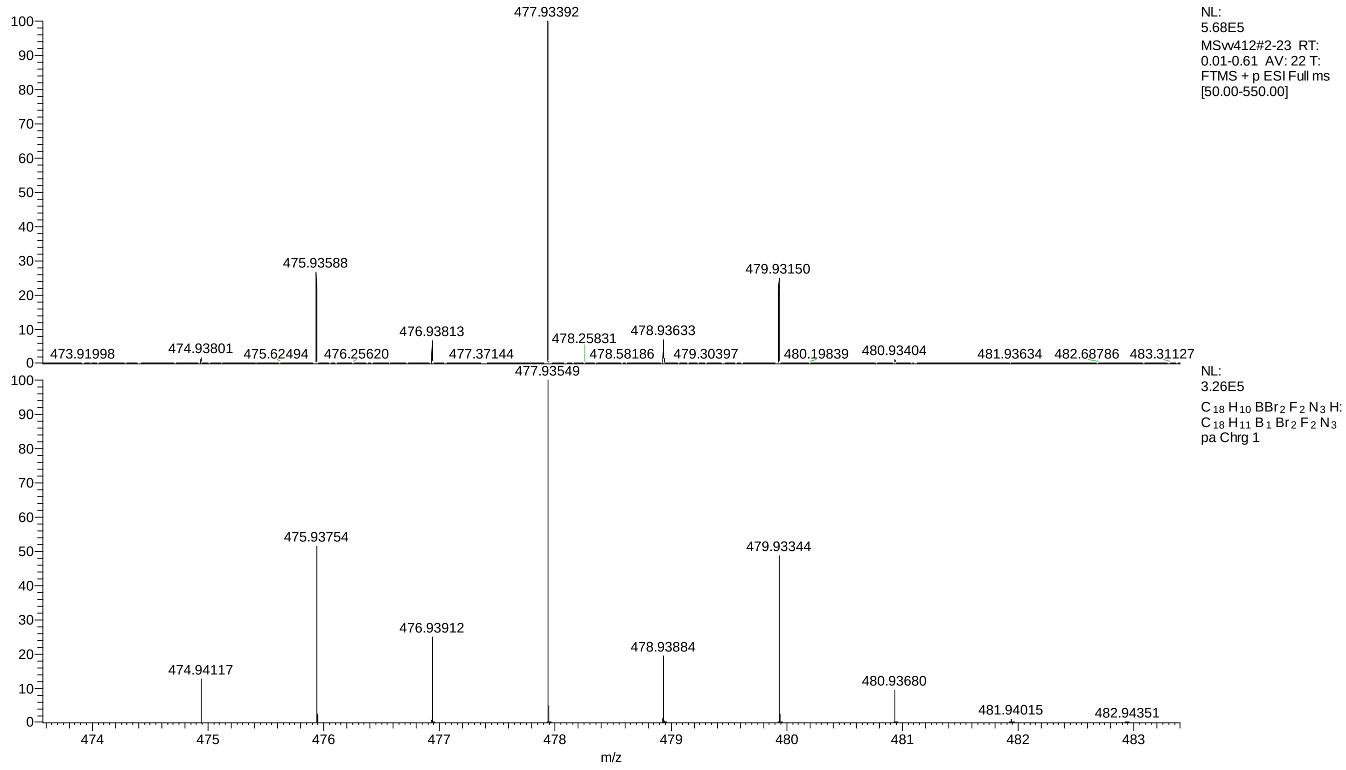
477.93392
NL:
5.68E5
MSw412#2-23 RT:
0.01-0.61 AV: 22 T:
FTMS + p ESI Full ms
[50.00-550.00]
475.93588
479.93150
476.93813
478.93633
478.25831
473.91998
474.93801
475.62494
476.25620
477.37144
478.58186
479.30397
480.19839
480.93404
481.93634
482.68786
483.31127
477.93549
NL:
3.26E5
C 18 H10 BBr2 F2 N3 H:
C 18 H11 B1 Br2 F2 N3
pa Chrg 1
475.93754
479.93344
476.93912
478.93884
474.94117
480.93680
481.94015
482.94351
100
90
80
70
60
50
40
30
20
10
0
474
475
476
477
478
479
480
481
482
483
m/z

S2 Singlet oxygen quantum yield

A 2.0 mL solution containing the photosensitizer (3 µM) along with 1,3-diphenylisobenzofuran (DPBF) as a singlet oxygen scavenger (120 µM) in pre-oxygenated DCM or CH_3CN was placed in a 2 mL cuvette. A 2.0 mL solution containing the photosensitizer (3 µM) was used as baseline. Thereafter, the photosensitizer + DPBF solutions were irradiated (λ_{irr} = 535 nm) with a UV/Vis-mounted Sahlmann Photochemical Solutions 535 nm LED system (peak wavelength = 535 nm, FWHM 32 nm). During 535 nm irradiation, the solutions' UV/Vis spectrum was monitored for the disappearance on the shoulder of the absorption band of DPBF at 441 nm, signifying consumption of the singlet oxygen acceptor by the generated singlet oxygen, to produce the graph shown below (measured as triplicates, single measurements shown in **Figure S2** –**Figure S5**). The rate of singlet oxygen formation was determined at the initial decay of absorbance of DPBF at 95% to 80% assuming every molecule of singlet oxygen is captured by the excess of scavenger present. The quantum yield (average of triplicate measurement) was calculated following the equations accordingly:

$$A = log_{10}\frac{I_0}{I} \qquad \text{where} \qquad I_0 = 1$$

Gives

$$I = \frac{1}{10^A}$$

Where A = absorbance of photosensitizer at $\lambda_{Irr,}$ I_0 = intensity incident light and I = transmitted intensity.

Following from the aforementioned equations the quantum yield for singlet oxygen formation (Φ_Δ) is defined as: [1]

$$\Phi_{\Delta\mathbf{BH1-2}} = \frac{I_{RB}}{I_{\boldsymbol{BH}\mathbf{1-2}}} \cdot \frac{k_{\boldsymbol{BH}\mathbf{1-2}}}{k_{RB}} \cdot \Phi_{\Delta\mathrm{RB}}$$

Where *k* = rate of scavenger consumption at λ_{Irr} and $\Phi_{\Delta RB}$ = 0.53 (lit. value).[2,3]

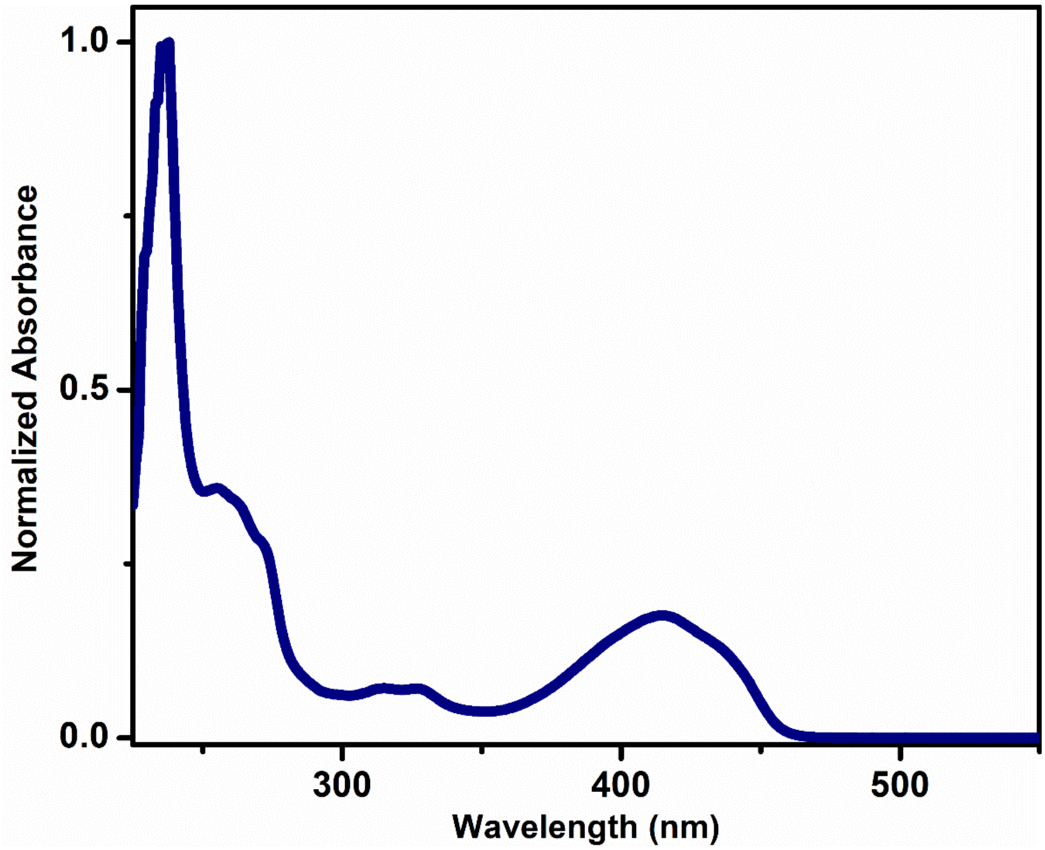

Figure S1 UV-Vis spectrum of DPBF (CH_3CN, 293 K).

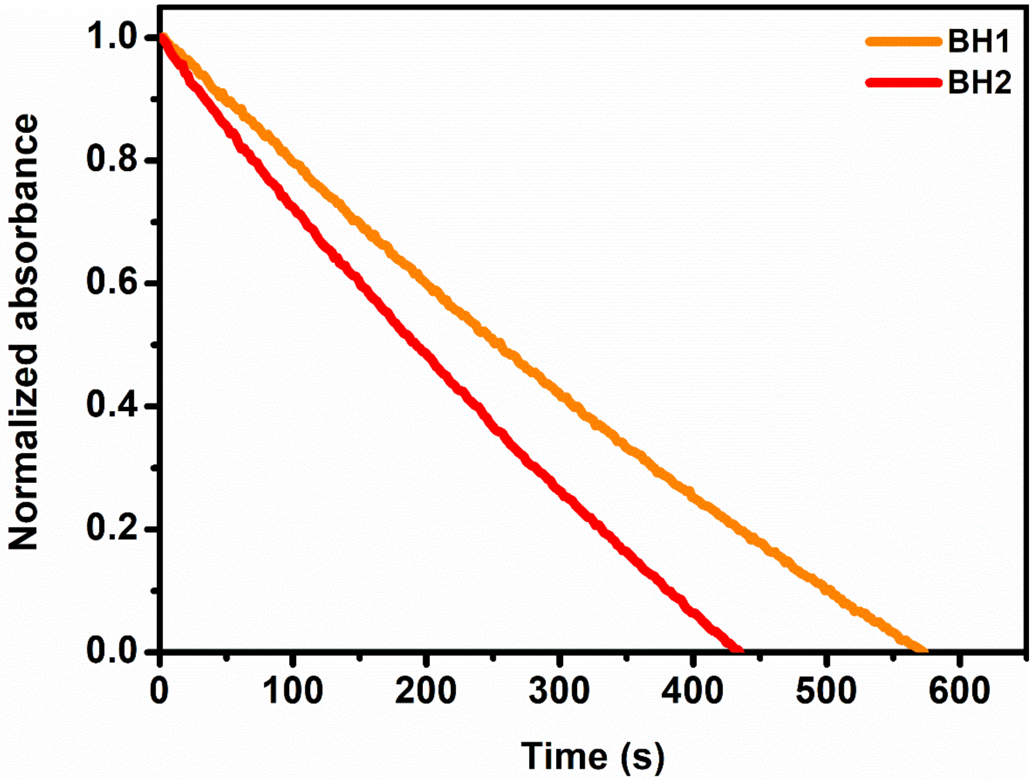

Figure S2 Decay of DPBF (120 µM) over time (s) monitored at λ = 441 nm in CH_3CN at 293 K.

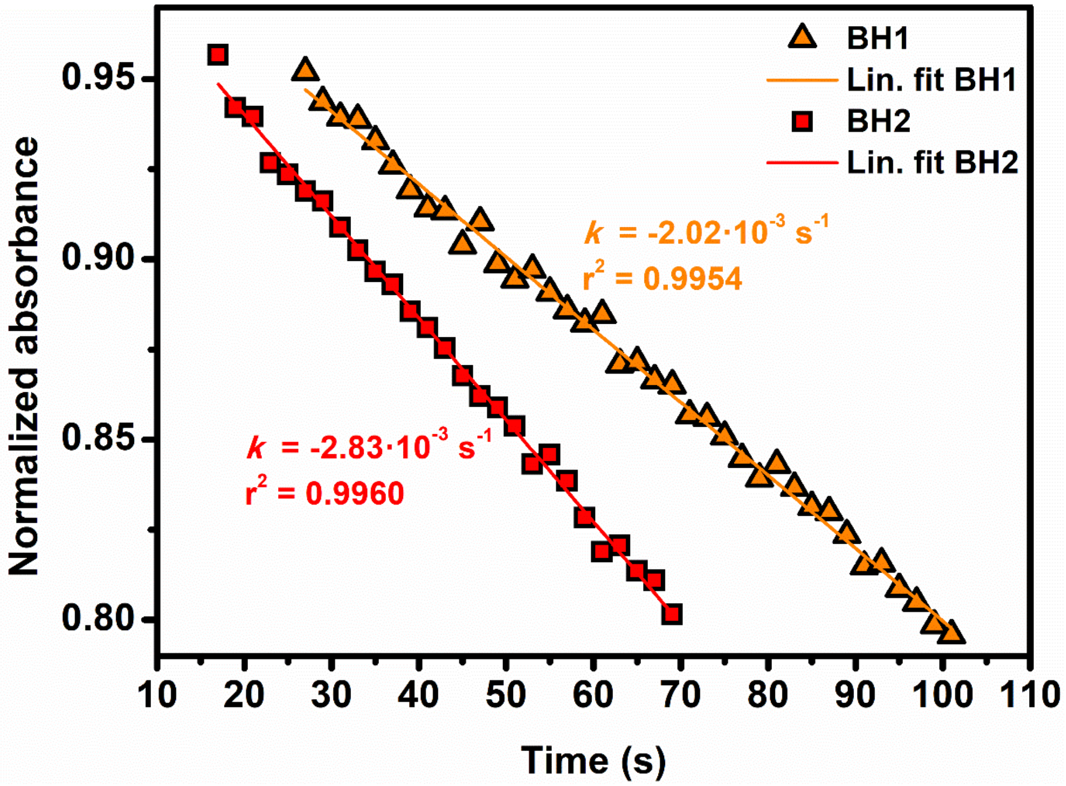

Figure S3 Rate of decay of DPBF (120 µM) over time (s) monitored at λ = 441 nm in CH_3CN at 293 K, measured from the initial decay at 95% to 80% absorbance.

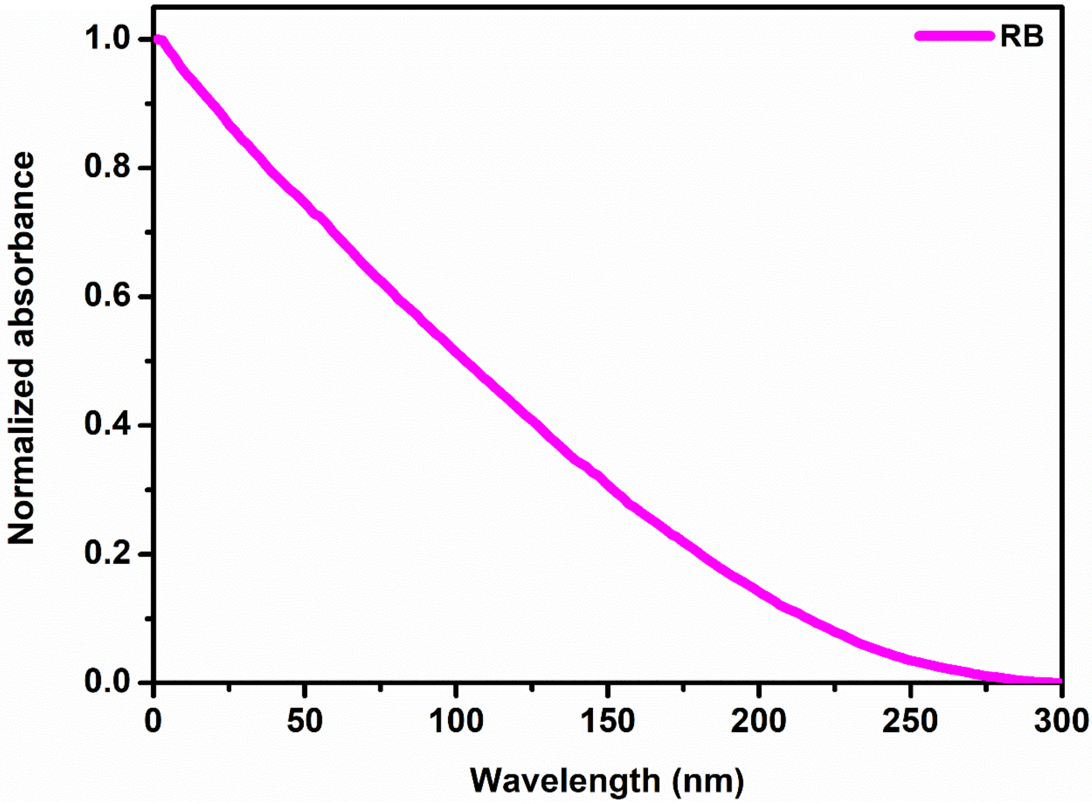

Figure S4. Decay of DPBF (120 µM) over time (s) monitored at λ = 441 nm in CH_3CN at 293 K

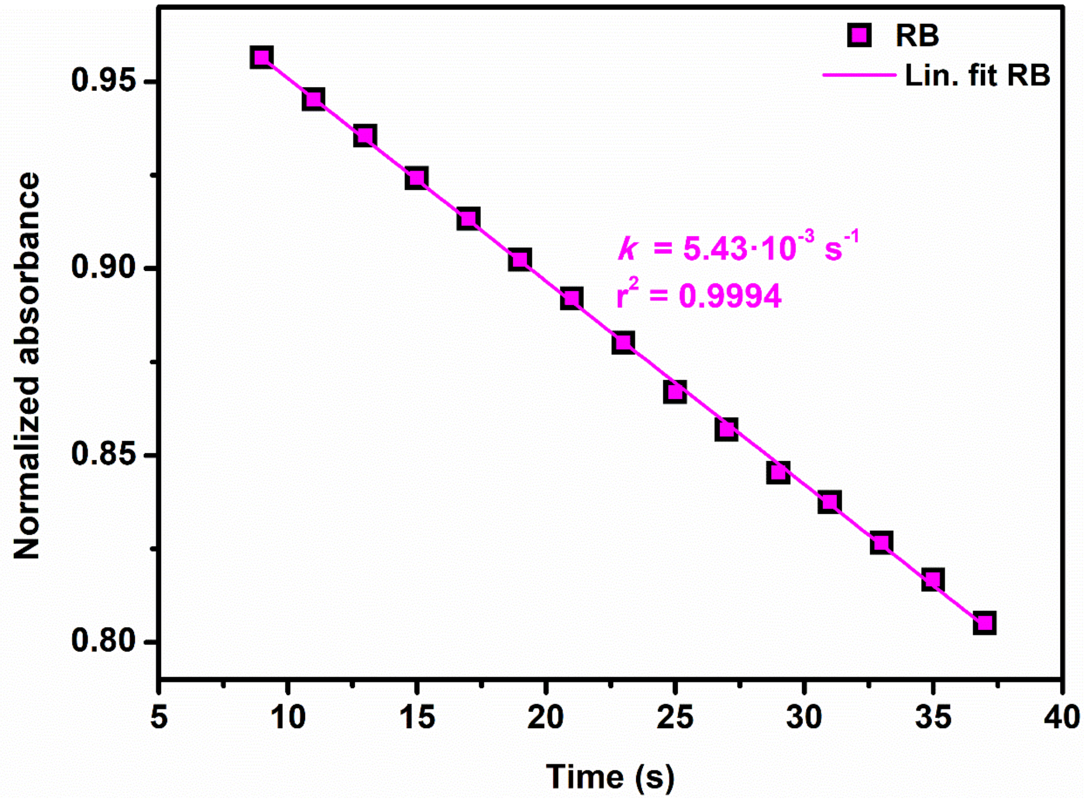

Figure S5. Rate of decay of DPBF (120 µM) over time (s) monitored at λ = 441 nm in CH_3CN at 293 K, measured from the initial decay at 95% to 80% absorbance.

S3 Photosensitizer Stability

The stability of the photosensitizers was measured by following the disappearance of the main absorption band of the photosensitizer in the absence of a scavenger (**BH1**: λ_{max} = 525 nm, **BH2**: λ_{max} = 519 nm). For comparison, the stability of Rose Bengal was determined in CH_3CN.

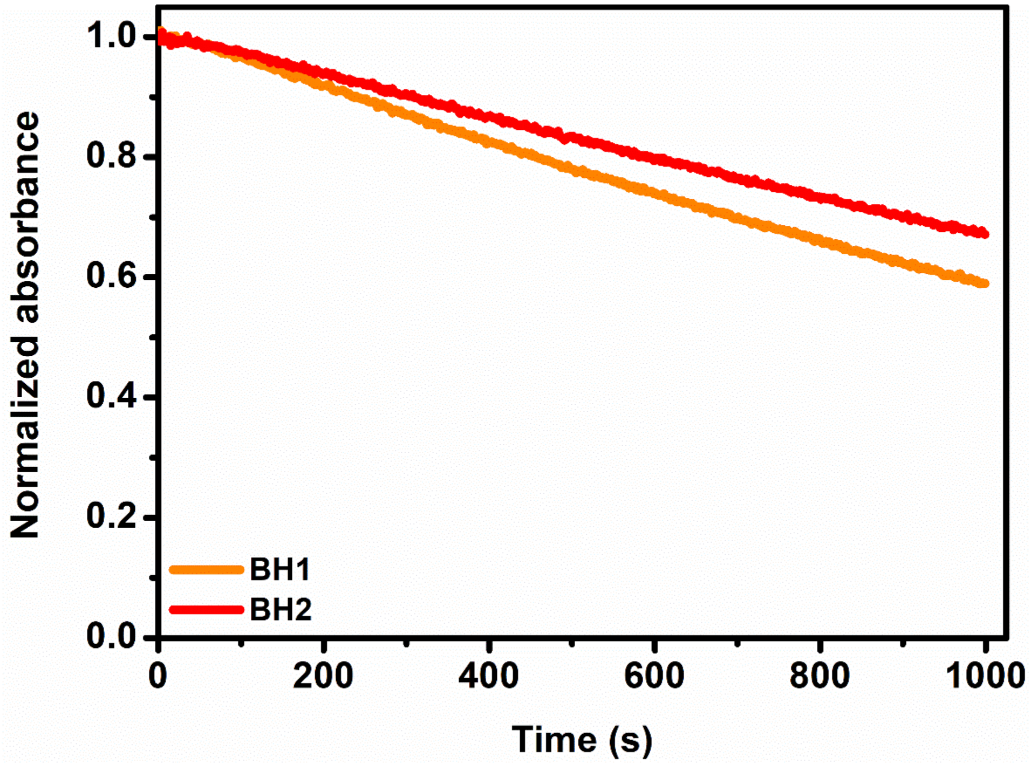

Figure S6 Decay of photosensitizers (3 µM) over time (s) monitored at the main absorption bands in CH_2Cl_2 at 293 K.

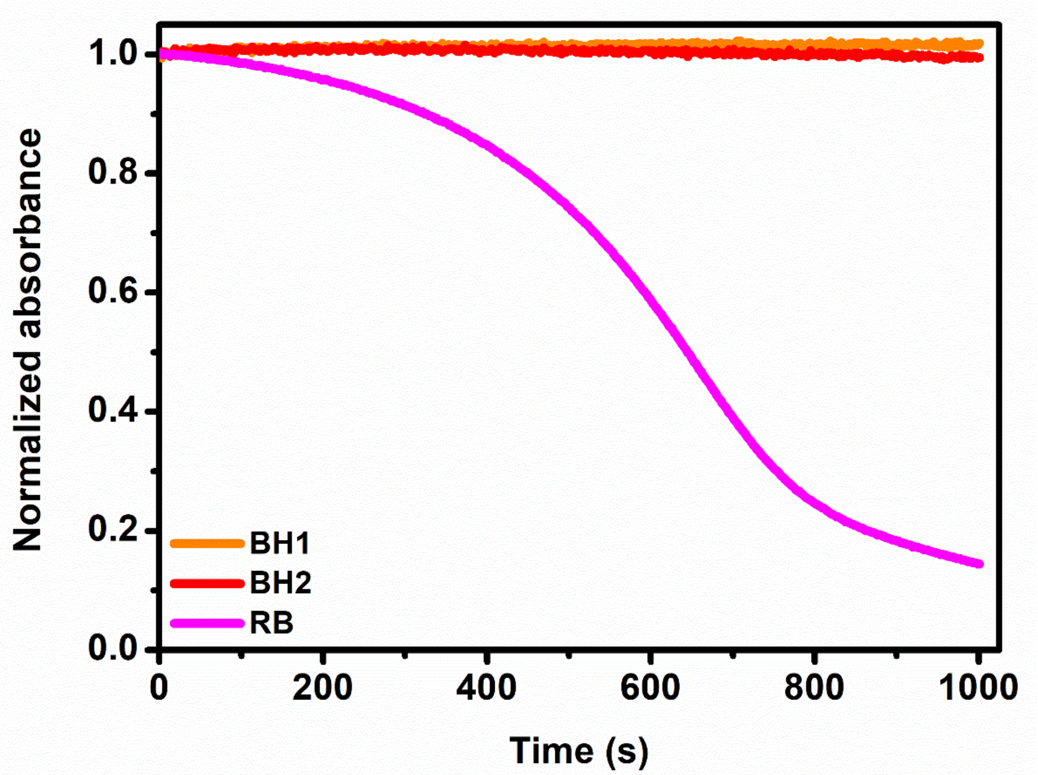

Figure S7 Decay of photosensitizers (3 µM) over time (s) monitored at the main absorption bands in CH_3CN at 293 K.

S4 Photosensitizer luminescence

A solution of the photosensitizer was prepared (3.0 ml, 3.0 µM in CH_2Cl_2) in a 3 ml cuvette to measure the emission wavelength and luminescence quantum yield Φ_{lum}. The emission spectrum (**Figure S8** – **Figure S9**) was recorded on an Edinburgh Instruments FS5 Steady State Spectrofluorometer with integrating sphere.

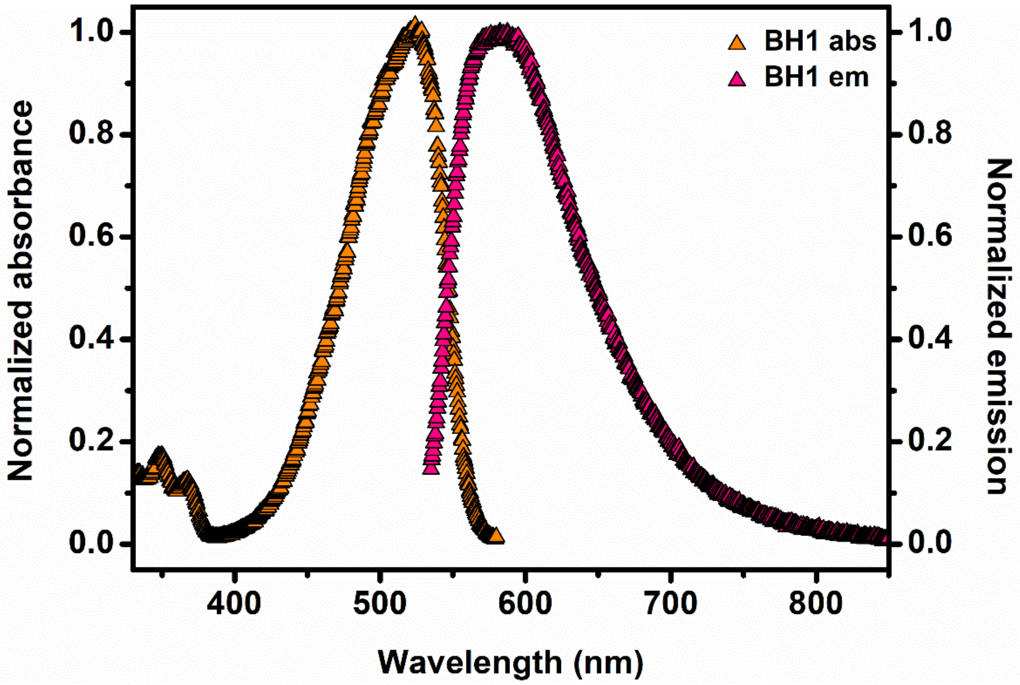

Figure S8 Normalized UV-Vis and emission spectrum of **BH1** (CH_2Cl_2, 293 K)

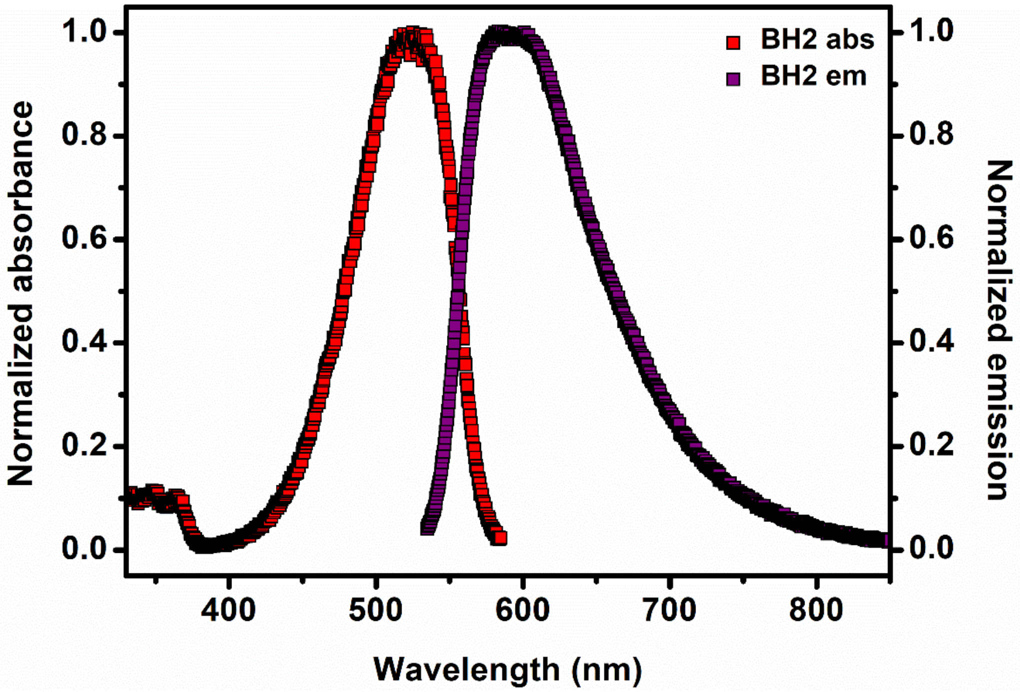

Figure S9 Normalized UV-Vis and emission spectrum of **BH2** (CH_2Cl_2, 293 K)

S5 Reaction kinetics photooxygenation

General experimental procedure photooxidation reaction kinetics

The model substrate (1.0 eq) and and photosensitizer (0.05 eq) were dissolved in the respective solvent (0.1 M), whereafter the mixture was irradiated at 293 K in a home-built irradiation setup (λ_{irr} = 514 nm) (**Figure S10**). At regular intervals a sample of 0.4 mL was taken from the reaction mixture, kept in darkness, dried in vacuo and dissolved in $CDCl_3$ for determination of the conversion by ^{1}H-NMR spectroscopy. The conversion was calculated by product : substrate ratio as all photooxidation reactions are selective.

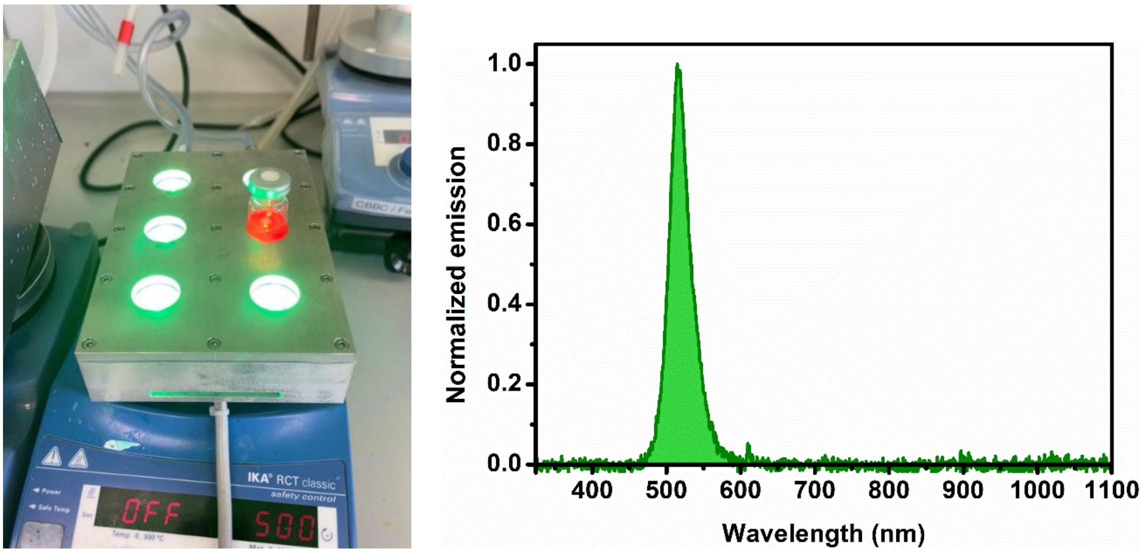

Figure S10 Home-built irradiation setup (left), normalized emission spectrum of green LED (right).

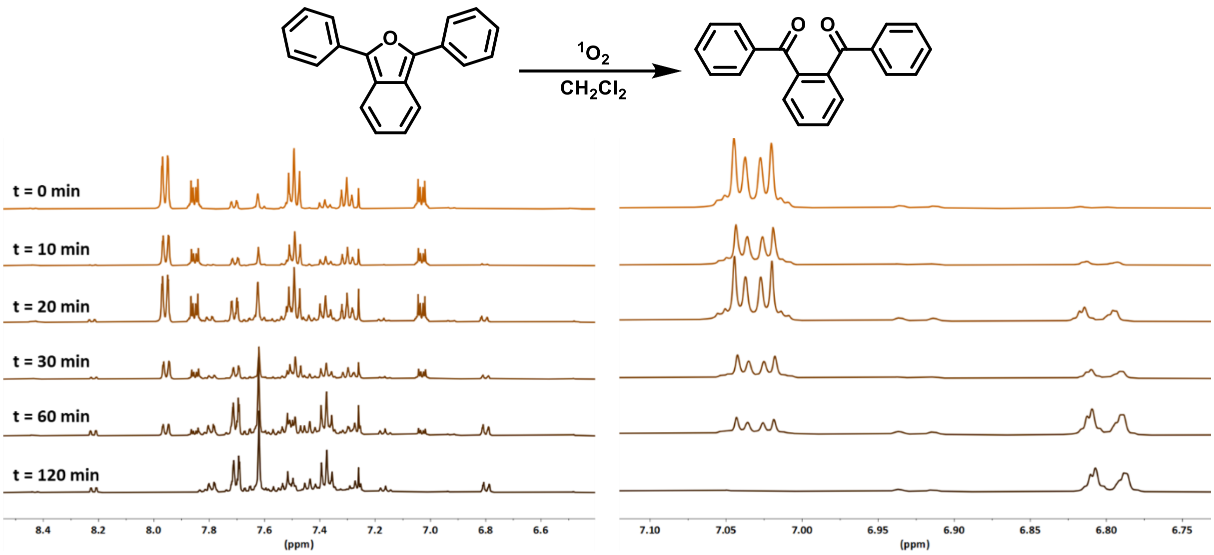

Figure S11 ^{1}H-NMR resonances over time indicating consumption of DPBF and production of 1,3-dibenzoylbenzene (left) using **BH1** as photosensitizer. Zoomed ^{1}H-NMR (right).

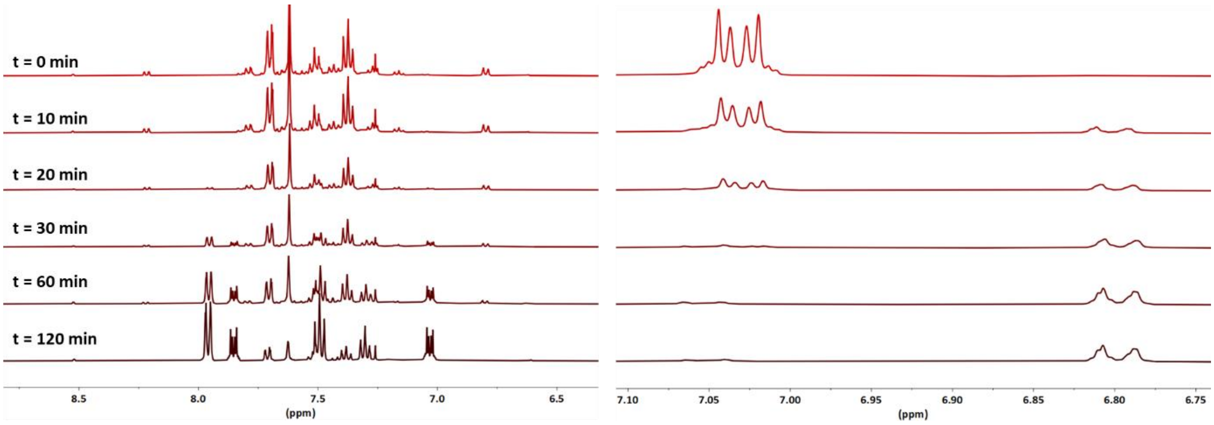

Figure S12 ^{1}H-NMR resonances over time indicating consumption of DPBF and production of 1,3-dibenzoylbenzene (left) using **BH2** as photosensitizer. Zoomed ^{1}H-NMR (right).

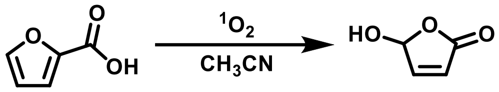

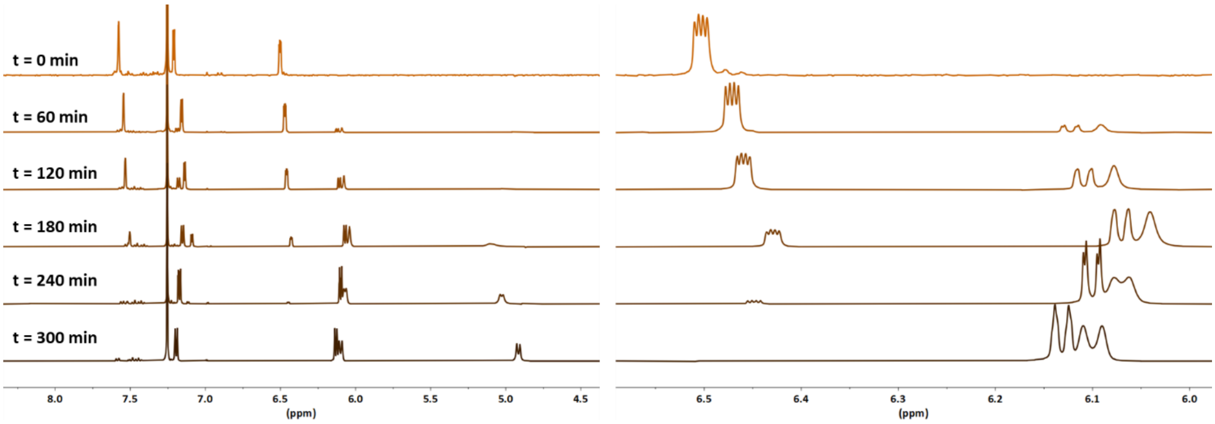

Figure S13 ^{1}H-NMR resonances over time indicating consumption of furoic acid and production of 5-hydroxyfuran-2(5H)-one (left) using **BH1** as photosensitizer. Zoomed ^{1}H-NMR (right).

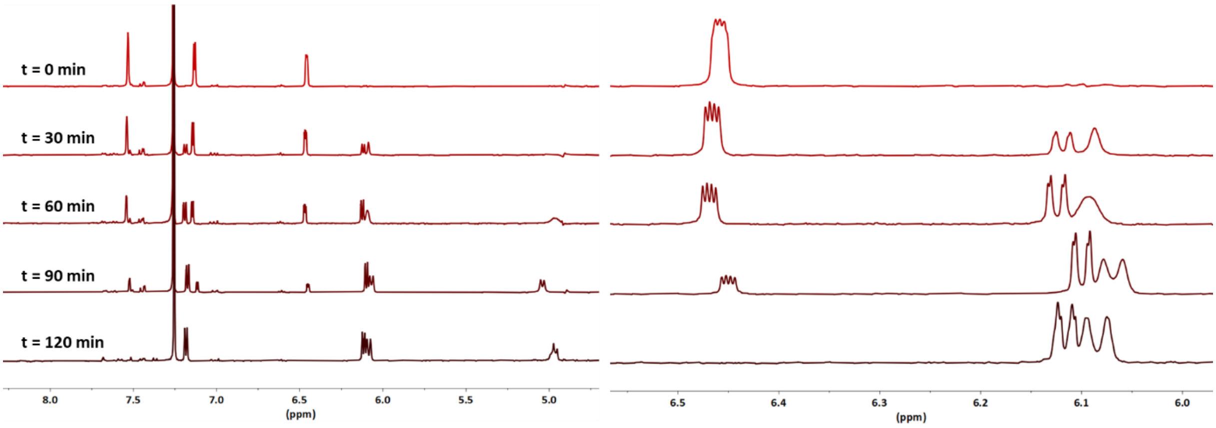

Figure S14 ^{1}H-NMR resonances over time indicating consumption of furoic acid and production of 5-hydroxyfuran-2(5H)-one (left) using **BH2** as photosensitizer. Zoomed ^{1}H-NMR (right).

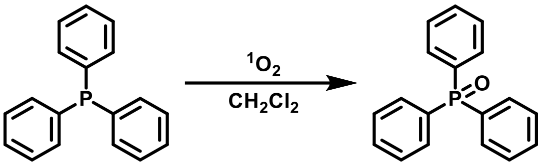

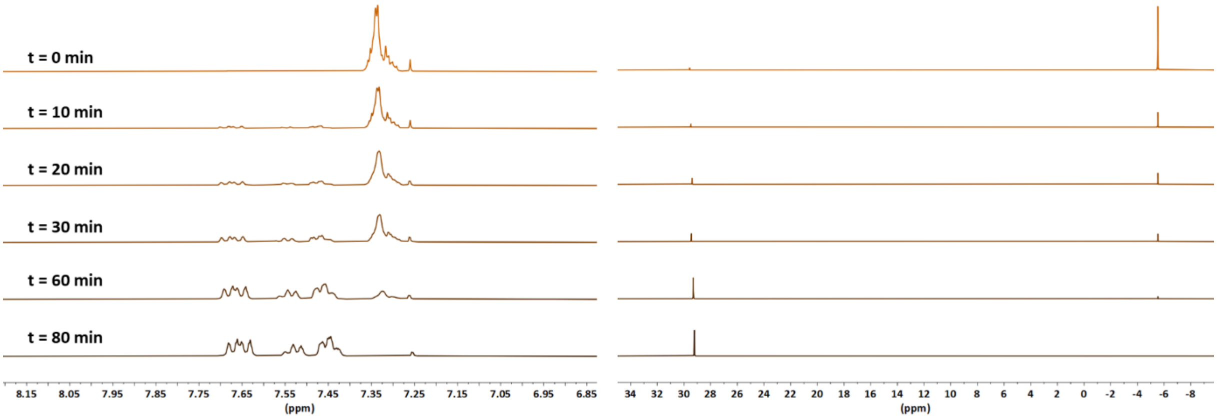

Figure S15 ^1H-NMR resonances over time indicating consumption of TPP and production of TPPO (left) using **BH1** as photosensitizer. ^{31}P-NMR (right).

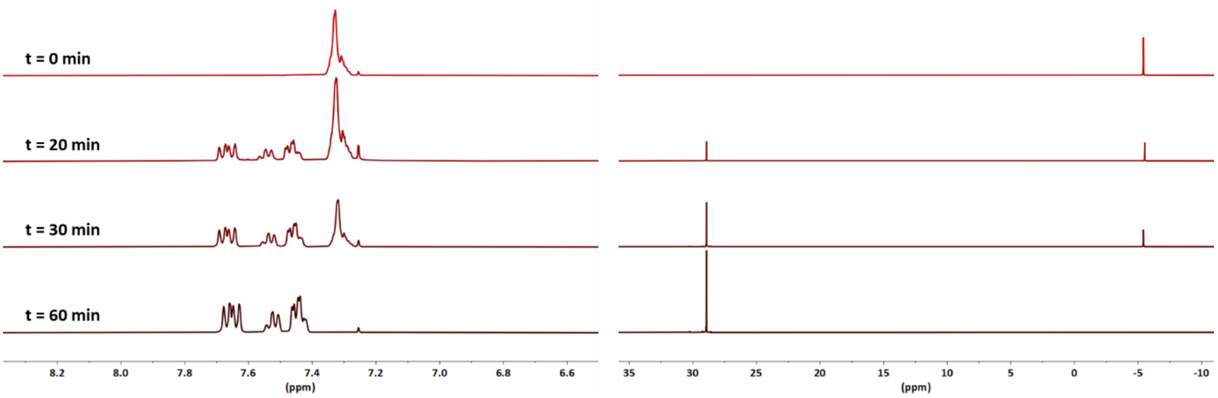

Figure S16 ^1H-NMR resonances over time indicating consumption of TPP and production of TPPO (left) using **BH2** as photosensitizer. ^{31}P-NMR (right).

S6 Preparative Scale Photooxygenation

A PhotoVap reactor[4] was used for the preparative 1 g photooxygenation of 2-FA, as it allows for efficient larger scale photooxygenation due the fast rotation creating a thin film, optimal for light penetration, and creating a high mass transfer of oxygen into the solution. To allow for an oxygen atmosphere in the rotary photoreactor, the photoreactor was purged with O_2 through vacuum/oxygen cycles using an O_2 filled balloon that was attached to the rotary evaporator. A home-built white light setup (575 lm, 8 W each; 5750 lm, 80 W total) consisting of standard white light LED bulbs was placed at a distance of approximately 5 cm around the 1 L flask, containing the reaction mixture (1.0 g 2-FA, 0.5 mol% **BH2**, 20 mL CH_3CN). After 6 h, the solvent was evaporated and the crude product was purified by column chromatography (SiO_2; Pentane / EtOAc 1:1) providing 5-hydroxyfuran-2(5H)-one in quantitative yield.

Figure S17. Rotary photoreactor in operation: Reaction conditions: 1 L flask, 1 g 2-FA in CH_3CN (20 mL),10 x 8W LED, 0.5 mol% **BH2.**

S7 Single Crystal X-ray Determination

Single-crystals were mounted on a cryoloop and placed in the nitrogen stream (100 K) of a Bruker-AXS D8 Venture diffractometer. Data collection and processing was carried out using the Bruker APEX3 software suite.[5,6] A multi-scan absorption correction was applied, based on the intensities of symmetry-related reflections measured at different angular settings (*SADABS*).[7] The structures were solved using *SHELXT*[8] and refinement was performed using *SHELXL*.[9] The hydrogen atoms were generated by geometrical considerations, constrained by idealized geometries and allowed to ride on their carrier atoms with an isotropic displacement parameter related to the equivalent displacement parameter of their carrier atoms.

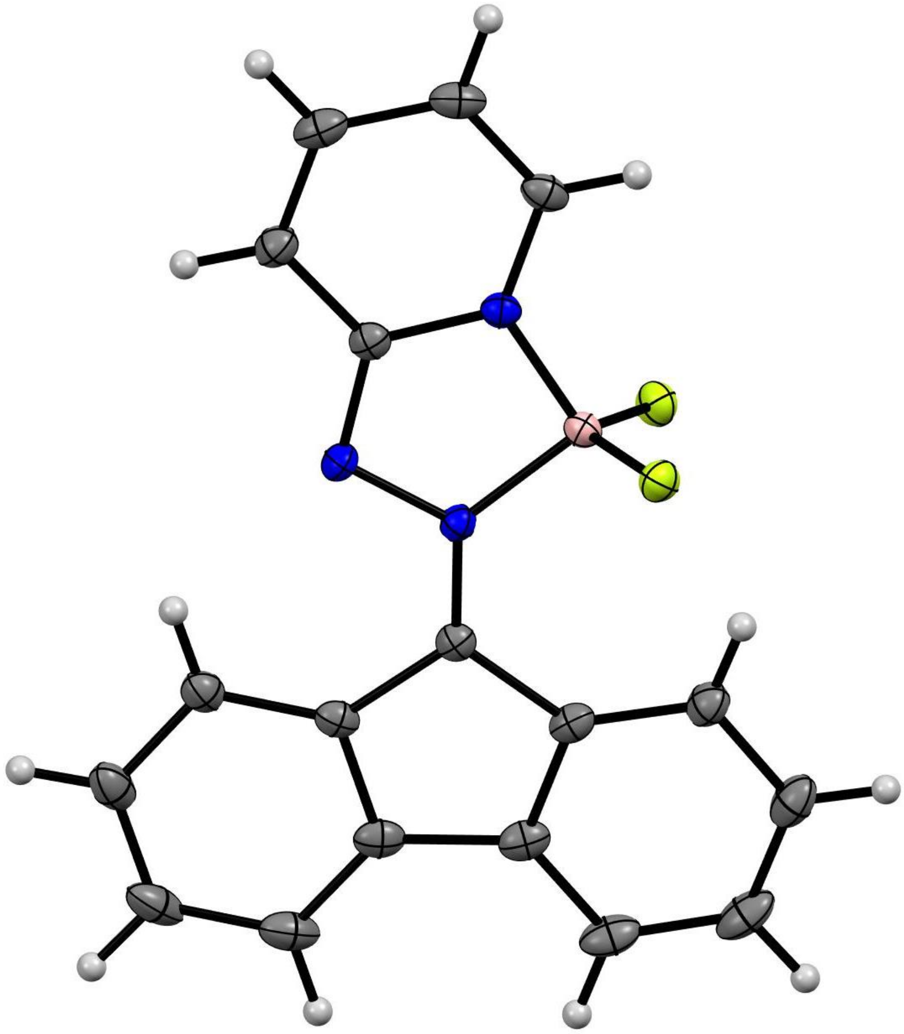

Figure S18 ORTEP image (ellipsoid at 50% probability) of complex **BH1.**

Name	**BH1**
Formula	$C_{18} H_{12} B_1 F_2 N_3$
Molecular Weight	319.12
Crystal System	monoclinic
T [K]	100(2)
Space Group	$P\ 2_1/n$
a [Å]	9.1067(3)
b [Å]	12.5882(4)
c [Å]	12.6809(4)
α [°]	90
β [°]	98.1690(10)
γ [°]	90
V [Å^3]	1438.95(8)
Z	4
D_{calc} [g·cm^{-3}]	1.473
Radiation [Å]	Cu K_α 1.54178
F(0 0 0)	656
h_{min}, h_{max}	–11, 11
k_{min}, k_{max}	–15, 15
l_{min}, l_{max}	–15, 15
μ [mm^{-1}]	0.885
Crystal Size [mm]	0.22 x 0.14 x 0.12
Colour, Shape	Lustrous dark red block
R_{int}	0.0281
ϑ_{min}, ϑ_{max} [°]	4.975, 74.470
Total Reflections (before merge)	27803
Data (I>3 x sigma(I)) [Reflections,Parameters,Restraints]	2944, 217, 0
S (=GooF)	1.046
Min. Residual Density [e/Å^3]	–0.240
Max. Residual Density [e/Å^3]	0.200
Threshold Expression	I>2sigma(I)
R_1	0.0356
wR_2	0.0793

References

1. L. V. Lutkus, S. S. Rickenbach and T. M. McCormick, *J. Photochem. Photobiol. A.,* 2019, **378**, 131 – 135.
2. W. P. Helman and A. B. Ross, *J. Phys. Chem. Ref. Data*, 1993, **22**, 113-262.
3. N.E. Elezcano, V. M. Martínez, E. P. Cabrera, C. F. A. G. Durán, I. L. Arbeloaa and S. Lacombec *RSC Adv*., 2016, **6**, 41991-41998.
4. C. A. Clark, D. S. Lee, S. J. Pickering, M. Poliakoff and M. W. George*, Org. Process Res. Dev*., 2016, **20**, 1792–1798*.*
5. Bruker, APEX3 (V2016.1-0), SAINT (Version 8.37A) and SADABS (Version 2014/5). Bruker AXS Inc., Madison, Wisconsin, USA.
6. Bruker, APEX3 (V2019.1-0), SAINT (Version 8.40A) and SADABS (Version 2016/1). Bruker AXS Inc., Madison, Wisconsin, USA.
7. L. Krause, R. Herbst-Irmer, G. M. Sheldrick and D. Stalke. *J. Appl. Crystallogr.,* 2015*,* **48**, 3–10.
8. G. M. Sheldrick, *Acta Crystallogr. Sect. A Found. Adv.*, 2015, **71**, 3–8.
9. G. M. Sheldrick, *Crystallogr Sect. A*, 2008, **64**, 112–122.